

## Preparation and Optical Properties of Substrates with Surface Nanostructure

V.P. Makhniy<sup>1,\*</sup>, G.I. Bodyl<sup>1</sup>, M.F. Pavlyuk<sup>2</sup>, O.M. Slyotov<sup>1,†</sup>

<sup>1</sup> Yuriy Fedkovych Chernivtsi National University, 2, Kotsubinskiy Str., 58012 Chernivtsi, Ukraine

<sup>2</sup> Vasyl Stefanyk Precarpathian National University, 57, Shevchenko Str., 76018 Ivano-Frankivsk, Ukraine

(Received 28 July 2017; published online 16 October 2017)

It is experimentally established that thermal annealing of single-crystal substrates of Cd<sub>1-x</sub>Mn<sub>x</sub>Te ( $x = 0.04-0.45$ ) solid solutions in the air at 920 K results in formation of surface nanostructure (SNS). In so doing, optimal annealing time  $t_a$  for each molar composition  $x$  is determined by empirical expression  $t_a \approx 35 + 1.3x$ , min. Analysis of AFM-topograms shows that SNS is a set of pyramids with the base size 2-5  $\mu\text{m}$ , which are a combination of smaller 10-100 nm nanopyramids. The result of size quantization in the latter is luminescence band in the energy region  $\hbar\omega$  larger than the energy gap of material  $E_g$ , and its maximum  $\hbar\omega_m$  with increasing  $x$  is displaced toward high-energy region. Large half-width of this band is due to considerable spread in dimensions of small nanopyramids. Displacement of maxima of bands of differential optical transmission spectra of substrates with SNS to low-energy region is explained by joint action of light absorption and scattering with participation of free pyramids.

**Keywords:** Cd<sub>1-x</sub>Mn<sub>x</sub>Te solid solutions, annealing, AFM-topograms, Surface nanostructure, Nanopyramids, Luminescence, Differential optical transmission spectra.

DOI: [10.21272/jnep.9\(5\).05026](https://doi.org/10.21272/jnep.9(5).05026)

PACS numbers: 61.46. – w, 68.37.Ps, 78.30.Fs, 78.55. – m

### 1. INTRODUCTION

The crystals of Cd<sub>1-x</sub>Mn<sub>x</sub>Te solid solutions have a bright outlook for the use in various fields of functional electronics, including devices with rectifying barrier. Among them are surface barrier diodes (SBD) which offer a number of advantages compared to rectifying structures with  $p-n$ -homo- or heterojunctions [1]. Besides, increase in Mn concentration causes the respective increase in bandgap  $E_g$  which contributes not only to expansion of spectral region of optoelectronic devices based on Cd<sub>1-x</sub>Mn<sub>x</sub>Te, but also to the increase in their temperature and radiation resistance. Unfortunately, growth of  $x$  leads to deterioration of the structural perfection of crystals, though solid solution is considered to be homogeneous up to  $x \approx 0.77$  [2]. The above structural defects can significantly degrade the operational parameters of devices on SBD and their temporal stability, as long as their properties are largely determined by the surface condition. In this connection, of great current interest is a search for methods and modes of treatment of semiconductor substrates for optimization of the basic surface parameters. One of the promising ways is creation of the surface nanostructure (SNS) which can not only improve characteristics of SBD, but also substantially change the properties of the base semiconductor. This paper is concerned with investigation of SNS influence on the optical properties of monocrystalline substrates of Cd<sub>1-x</sub>Mn<sub>x</sub>Te solid solutions.

### 2. SAMPLES AND INVESTIGATION TECHNIQUES

Note that at present the only known method for obtaining SNS on Cd<sub>1-x</sub>Mn<sub>x</sub>Te substrates is their processing with pulsed radiation of a ruby laser. Thus, in

papers [3-5] it was shown that irradiation of CdTe and Cd<sub>0.96</sub>Mn<sub>0.04</sub>Te samples by light impulses with energy density below the ablation threshold leads to the formation of nanosized ordered structures on the surface. The average arithmetic roughness and homogeneity of the islets are determined by the energy and time of irradiation and in general they are complex in nature which is explained by defect-deformation mechanism of the phase transition on the surface of the crystals.

For creation of SNS we used a much simpler technology which successfully showed itself in the manufacture of Au-CdTe contacts with the efficiency of photo transformation  $\sim (13-15)\%$  at 300 K in light conditions AM1.5 [6]. It is based on self organization processes that are realized in narrow temperature and time intervals of annealing of semiconductor substrates in the air. Instead, it was found that the regimes given in [7] for CdTe were completely unsuitable for Cd<sub>1-x</sub>Mn<sub>x</sub>Te samples. In this regard, the optimal values of the temperature  $T_a$  and the time of annealing  $t_a$  were determined experimentally by the similarity of AFM-topogram of each solids composition to AFM-topogram of CdTe (Fig. 1), in which the maximum efficiency of the photoluminescence is observed [7]. Studies have shown that temperature  $T_a \approx 650 \pm 20^\circ\text{C}$  corresponds to these criteria for Cd<sub>1-x</sub>Mn<sub>x</sub>Te. Time  $t_a$  depends on molar composition and is well described by the empirical formula  $t_a = 35 + 1.3x$ , min, Fig. 2. It was also experimentally determined that temperature  $T_a \approx 650 \pm 20^\circ\text{C}$  is optimal, because at  $T < T_a$  the surface remains almost specular, while at  $T > T_a$  it tends to form a block structure. In addition, studies have shown that the formation of SNS on the Cd<sub>1-x</sub>Mn<sub>x</sub>Te substrates, as in the case of CdTe, causes a significant increase in the efficiency of luminescent radiation, the nature of which is discussed below.

\* [vpakhniy@gmail.com](mailto:vpakhniy@gmail.com)

† [o.slyotov@chnu.edu.ua](mailto:o.slyotov@chnu.edu.ua)

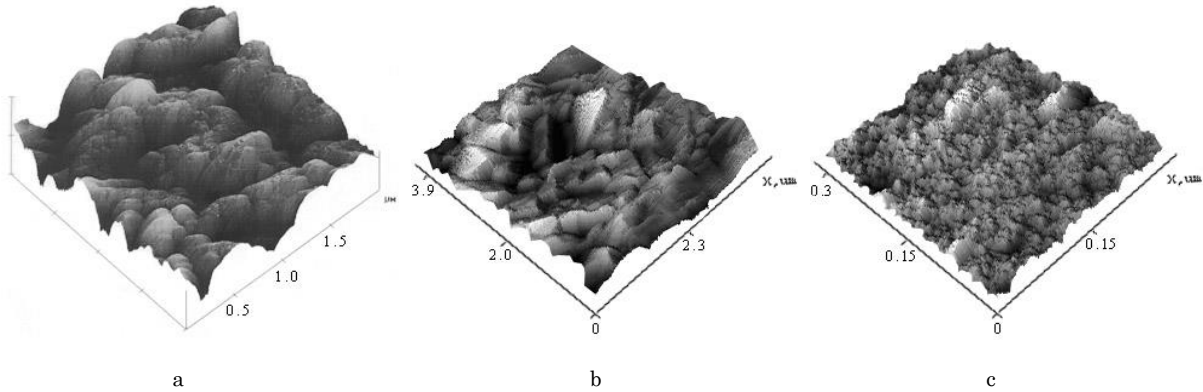


**Fig. 1** – AFM-topogram of the surface fragments of CdTe (a) and Cd<sub>1-x</sub>Mn<sub>x</sub>Te (b, c) substrates annealed under optimal conditions

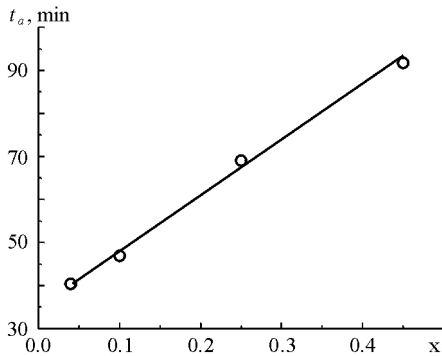


**Fig. 2** – Dependence of annealing time  $t_a$  on molar composition  $x$  of Cd<sub>1-x</sub>Mn<sub>x</sub>Te crystals annealed at  $T_a \approx 620$  °C

Surface morphology was studied with the use of atomic-force microscope NT-206, and AFM-topogram of CdTe and Cd<sub>1-x</sub>Mn<sub>x</sub>Te samples annealed under optimal conditions are presented in Fig. 1. Luminescent spectra  $N_\omega$  and optical transmission spectra  $T_\omega$  were investigated using a universal measuring complex consisting of a diffraction MDR-23 monochromator and standard synchronous detection system. Photoluminescence was excited by N<sub>2</sub>-laser with a wavelength  $\lambda_m \approx 0.337$  μm, and a photomultiplier FEP-79 was used as a detector. A change in excitation level  $L$  within four orders of magnitude was performed with the aid of a calibrated set of neutral-density filters. A halogen lamp with “smooth” radiation spectrum served to measure the differential transmission spectra  $T'_\omega$ , and the measurements were carried out on the same complex in  $\lambda$ -modulation mode [8]. The spectral characteristics were plotted with regard to the corresponding hardware functions of the measuring complex, and the studies were conducted in the room temperature range.

### 3. RESULTS AND DISCUSSIONS

The most characteristic feature of the Cd<sub>1-x</sub>Mn<sub>x</sub>Te substrates annealed under optimal conditions is the appearance of  $B$ -band (Fig. 3) which has the following properties. First of all, it has a rather big half-width ( $\Delta\hbar\omega_z \approx 0.8$  eV) that practically does not depend on the molar composition  $x$  of substrates and the excitation level  $L$ . Second, the energy position of the maximum  $\hbar\omega_m^B$  significantly exceeds  $E_g$  of the base material and

increases with increasing of  $x$ , inset in Fig. 3. Third, its intensity  $I_B$  depends linearly on the excitation level within four orders of magnitude. All these facts exclude the participation in the formation of  $B$ -band of  $\beta$ -MnTe clusters, the radiation of which in Cd<sub>1-x</sub>Mn<sub>x</sub>Te crystals at 300 K is characterized by the following parameters –  $\hbar\omega_m \approx 3.24$  eV,  $\Delta\hbar\omega_z \approx 0.06$  eV and  $I \sim L^2$  [9]. Also, note that the luminescence of the  $\beta$ -MnTe clusters was observed only at excitation levels 3-5 orders of magnitude larger than the maximum value  $L$  used in this paper. Finally, we note that  $B$ -band is not formed by transitions between conduction band and the valence band split due to the spin-orbital interaction, because in this case parameter  $\Delta\hbar\omega_z$  would be  $\sim 0.05$  eV and the dependence  $I(L)$  should obey the law  $I \sim L^2$  [10].

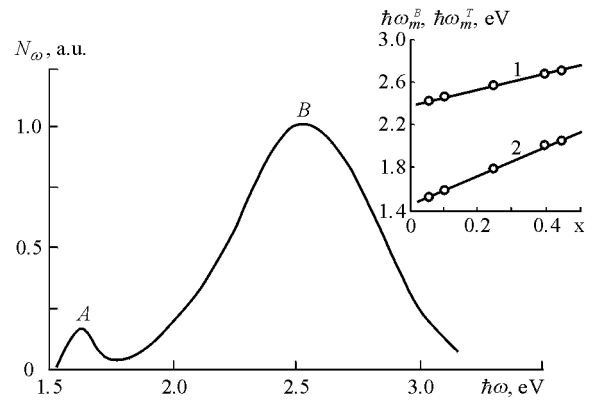


**Fig. 3** – Photoluminescence spectrum of Cd<sub>0.75</sub>Mn<sub>0.25</sub>Te substrate with SNS. On the inset – the dependence of  $B$ -band maxima position (1) and differential optical transmission (2) of the base substrate on molar composition.  $T = 300$  K

Taking into account the above, the most likely reason for the occurrence of  $B$ -band is SNS, which appears after annealing of the substrates under optimal conditions. It is here that quantum-size effect is realized, which becomes apparent in increasing the bandgap of spherical crystal as compared to unbounded. If we consider that luminescence is caused by a set of oscillators, their largest number is responsible for radiation with the energy  $\hbar\omega_m$ , which can be represented by expression [11]

$$\hbar\omega_m^B = E_g + \frac{\pi^2 \hbar^2}{2d_0} \left( \frac{1}{m_n^*} + \frac{1}{m_p^*} \right). \quad (1)$$

Where  $d_0$  is diameter of spherical nanocrystal,  $m_n^*$  and  $m_p^*$  are effective masses of electron and hole, respectively. As long as the bandgap of  $\text{Cd}_{1-x}\text{Mn}_x\text{Te}$  solid solutions is a linear function of  $x$  [12], then according to (1) in the first approximation  $\hbar\omega_m^B$  should be also similar to dependence  $E_g(x)$ . Indeed, experimental dependence  $\hbar\omega_m^B(x)$  is approximated by a straight line at  $x$  change within 0.04-0.45. However, its slope is almost factor of two smaller than that of dependence  $E_g(x)$ , inset in Fig. 3. Possible reasons for such distinctions will be discussed later.

Formula (1) allows estimating the average size of nanocrystals that determine the maximum of  $B$ -band. Due to the absence of information on dependences  $m_{n,p}^*(x)$  for  $\text{Cd}_{1-x}\text{Mn}_x\text{Te}$  solid solution and taking to account the estimative nature of the calculations, we will use the known value of  $m_n^* = 0.1m_0$  and  $m_p^* = 0.35m_0$  for CdTe [13]. Assuming the average value of the difference  $\hbar\omega_m^B - E_g \approx 0.7$  eV and after the substitution of the quantities  $m_{n,p}^*$  we will obtain for  $d_0 \approx 5$  nm. Instead, the analysis of zoomed fragment of AFM-topogram (Fig. 1c) shows that the minimal size of pyramids SNS is  $\sim 10$  nm, which is twice as large as the estimated value. The contradiction is eliminated, if we assume that the radiation in the vicinity of the maximum of  $B$ -band is formed by the vertices of nanopyramids. The collateral evidence is presence in the luminescence spectrum of photons with the energies  $\hbar\omega > \hbar\omega_m$ , which may be due to nanoobjects of size smaller than  $d_0 \approx 5$  nm. An abnormally large half-width of  $B$ -band is caused by significant dispersion of sizes (10-100 nm) of shallow nanocrystals that are part of the larger pyramids with the base size 1-5  $\mu\text{m}$ , Fig. 1c.

As will be shown below, larger size structural elements of SNS taking no part in the formation of  $B$ -band cause significant changes in optical transmission. We will analyze the results involving differential transmission spectra  $T'_\omega$  used to find dependence  $E_g(x)$  of  $\text{Cd}_{1-x}\text{Mn}_x\text{Te}$  base substrates, inset in Fig.3. The value  $E_g$  for each composition was determined by the energy position of maximum  $\hbar\omega_m^T$  of curve  $T'_\omega$ , typical appearance of which for  $\text{Cd}_{0.75}\text{Mn}_{0.25}\text{Te}$  is presented by curve 1 in Fig. 4.

Due to the fact that the position of  $\hbar\omega_m^T$  (hence, the value of  $E_g$ ) depends not only on  $x$  but also on sample thickness  $l$ , the latter for all base substrates was identical and equal to 200  $\mu\text{m}$ . It is obvious from the above that the experimental values  $E_g(l)$  will be different from real  $E_g(0)$ , and the difference  $\Delta E_g = E_g(l) - E_g(0)$  will also depend on  $l$  and grow as the thickness increases. Instead, for substrates of cadmium telluride (which, like a solid solution, is a direct-gap semiconductor) of thickness  $\sim 200$   $\mu\text{m}$ , the  $\Delta E_g \sim 30$  meV [14]. In so doing, the relative error  $\Delta E_g/E_g$  in determining the

bandgap from the curves  $T'_\omega$  of  $\text{Cd}_{1-x}\text{Mn}_x\text{Te}$  ( $0.04 \leq x \leq 0.45$ ) substrates does not exceed 0.02 with little or no impact on the absolute value of  $E_g$  and its dependence on  $x$ . So, we can assume that the reason for the difference in the slope of the straight lines (inset in Fig. 3) is dependence of  $m_{n,p}^*$  and  $d_0$  on  $x$ , the definition of which goes beyond the scope of this work.

Research showed that creation of SNS on the substrates causes a decrease in the ordinate of curve  $T'_\omega$  and also a shift of its maximum  $\hbar\omega_m^T$  towards lower energies, Fig. 4.

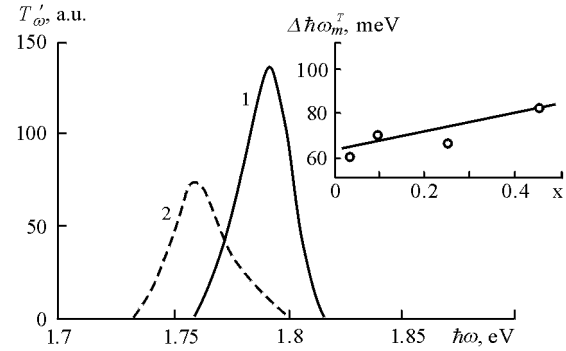


**Fig. 4** – Differential spectra of optical transmission of  $\text{Cd}_{0.75}\text{Mn}_{0.25}\text{Te}$  substrates: with SNS (2) and without (1). On the inset – the dependence of the difference in maxima position of curves  $T'_\omega$  of the base crystals and crystals with SNS on molar composition.  $T = 300$  K

Note that this fact is observed for all samples under study. Moreover, the difference  $\hbar\omega_m^T$  between curve maxima  $T'_\omega$  of specular and matt surfaces grows with the increase in  $x$ , inset in Fig. 4. These results are consequence of light scattering effect on pyramids of different size  $d$ , including with  $d \leq 0.1-0.2\lambda_0$ . The wavelength  $\lambda_0$  corresponds to the absorption edge and is determined by formula  $\lambda_0 = 1.24/E_g$ , varying for the investigated samples in the range of 600-800 nm. For structural elements with such  $d$  in the first approximation it can be considered that the intensity of scattered light  $I_d$  changes by the Rayleigh law  $I_d \sim \omega^4$ , which causes an increase in the absorption and the observed shift of  $\hbar\omega_m^T$ . Decrease in the ordinates of curves  $T'_\omega$  of substrates with SNS compared to non-annealed substrates (Fig. 4) is due to increase in absorption coefficient, which is related to multiple reflection processes on pyramids with  $d_0 \approx 1-5$   $\mu\text{m}$ . Such effects are observed in textured Si-photolements [15], as well as in Au-CdTe contacts with a modified surface [6], eventually causing significant improvement of their photoelectric parameters. Besides, as in the case of CdTe [7], SNS leads to decrease in the speed of surface recombination. This results in efficiency increase of  $A$ -band boundary photoluminescence (Fig. 3) which is almost two orders of magnitude smaller in the base substrates.

#### 4. CONCLUSIONS

Thus, the above results indicate the possibility of obtaining the surface nanostructure on  $\text{Cd}_{1-x}\text{Mn}_x\text{Te}$

substrates by annealing under certain conditions in the air. AFM-topograms show that surface nanostructure consists of pyramids of size 2-5  $\mu\text{m}$  which in turn are a combination of smaller 10-100 nm nanopyrramids. The latter participate in the formation of a wide band of photoluminescence in the region of photon energy 2.2-

3.2 eV, which is the result of quantum-size effects. The structural elements of larger size are responsible for the observed shift towards the low-energy region of maxima of differential optical transmission spectra and the decrease in their amplitude.

### Отримання та оптичні властивості підкладинок з поверхневою наноструктурою

В. П. Махній<sup>1</sup>, Г. І. Бодюл<sup>1</sup>, М. Ф. Павлюк<sup>2</sup>, О. М. Сльотов<sup>1</sup>

<sup>1</sup> Чернівецький національний університет імені Юрія Федьковича, вул. Коцюбинського 2, 58012 Чернівці, Україна

<sup>2</sup> Прикарпатський національний університет імені Василя Стефаника, вул. Шевченка 57, 76018 Івано-Франківськ, Україна

Експериментально встановлено, що термічний відпал монокристалічних підкладинок твердих розчинів  $\text{Cd}_{1-x}\text{Mn}_x\text{Te}$  ( $x = 0,04-0,45$ ) на повітрі при  $650^\circ\text{C}$  приводить до утворення поверхневої наноструктури (ПНС). При цьому оптимальний час відпалу  $t_b$  для кожного молярного складу  $x$  визначається емпіричним виразом  $t_b \approx 35 + 1,3x$ , хв. Аналіз АСМ-топограм показує, що ПНС являє собою набір пірамід з розміром основи 2-5 мкм, які є об'єднанням більш мілких 10-100 нм нанопірамід. Наслідком розмірного квантування в останніх є смуга люмінесценції в області енергій  $\hbar\omega$  більших за ширину забороненої зони  $E_g$  матеріалу, а її максимум  $\hbar\omega_m$  з ростом  $x$  зміщується у високоенергетичну сторону. Велика півширина цієї смуги обумовлена значним розкидом розмірів мілких нанопірамід. Зміщення максимумів смуг диференційних спектрів оптичного пропускання підкладинок з ПНС у низькоенергетичну область пояснюється сумісною дією процесів поглинання і розсіяння світла за участю більших пірамід.

**Ключові слова:** Тверді розчини  $\text{Cd}_{1-x}\text{Mn}_x\text{Te}$ , Відпал, Поверхнева наноструктура, АСМ-топограми, нанопіраміди, Люмінесценція, Диференційні спектри оптичного пропускання.

### Получение и оптические свойства подложек с поверхностной наноструктурой

В. П. Махний<sup>1</sup>, Г. И. Бодюл<sup>1</sup>, М. Ф. Павлюк<sup>2</sup>, А. М. Слётов<sup>1</sup>

<sup>1</sup> Черновицкий национальный университет имени Юрия Федьковича, ул. Коцюбинского 2, 58012 Черновцы, Украина

<sup>2</sup> Прикарпатский национальный университет имени Василия Стефаника, ул. Шевченка 57, 76018 Ивано-Франковск, Украина

Експериментально встановлено, що термічний отжиг монокристалічних підложек твердих розчинів  $\text{Cd}_{1-x}\text{Mn}_x\text{Te}$  ( $x = 0,04-0,45$ ) на повітрі при  $650^\circ\text{C}$  приводить до утворення поверхневої наноструктури (ПНС). При цьому оптимальне час отжига  $t_o$  для кожного молярного складу  $x$  визначається емпіричним виразом  $t_o \approx 35 + 1,3x$ , мин. Аналіз АСМ-топограм показує, що ПНС являє собою набір пірамід з розміром основи 2-5 мкм, які є об'єднанням більш мілких 10-100 нм нанопірамід. Следствием розмірного квантування в останніх є смуга люмінесценції в області енергій  $\hbar\omega$  більших за ширину забороненої зони  $E_g$  матеріалу, а її максимум  $\hbar\omega_m$  з збільшенням  $x$  зміщується у високоенергетичну сторону. Велика півширина даної смуги обумовлена значительним розбросом розмірів мілких нанопірамід. Зміщення максимумів смуг диференційних спектрів оптичного пропускання підложек з ПНС у низькоенергетичну область пояснюється сумісним дією процесів поглинання і розсіяння світла з участю вільних пірамід.

**Ключевые слова:** Твердые растворы  $\text{Cd}_{1-x}\text{Mn}_x\text{Te}$ , Отжиг, Поверхностная наноструктура, АСМ-топограммы, Нанопирамиды, Люминесценция, Дифференциальные спектры оптичного пропускання.

### REFERENCES

1. K.A. Valiev, Yu.I. Pashuntsev, G.V. Petrov, *Application of Metal-Semiconductor Contacts in Electronics* (Moscow: Radio i Svyaz: 1980).
2. V.F. Agekyan, N.G. Filosofov, *Diluted Magnetic Semiconductors* (S-Pb, 2014).
3. A. Baidullaeva, A.I. Vlasenko, L.F. Cuzan, O.S. Litvin, P.E. Mozol', *Semicond.* **39** No 9, 1028 (2005).
4. V.I. Emel'yanov, A. Baidullaeva, A.I. Vlasenko, L.F. Kuzan, O.S. Lytvyn, P.E. Mozol', *Techn. Phys. Lett.* **32** No 8, 732 (2006).
5. A. Baidullaeva, A.I. Vlasenko, E.I. Gatskevich, V.A. Gnatyuk, G.D. Ivlev, and P.E. Mozol', *Nanosist., Nanomat., Nanotechnol.* **6** No 4, 1167 (2008).
6. R. Ciaha, M.V. Demich, P.M. Gorley, Z. Kuzhicki, V.P. Makhniy, I.V. Malimon, Z. Swiaten, *J. Cryst. Growth* **197**, 675 (1999).

7. V.P. Makhniy, I.I. German, E.I. Tchernykh, *J. Surf. Investig.: X-ray, Synchrotron Neutron Techn.* **7**, 562 (2013).
8. V.P. Makhniy, *Principles and Methods of Modulation Spectroscopy* (Chernivtsi: Ruta, 2001).
9. I.G. Aksyanov, M.E. Kompan, M.V. Mesh, *Phys. Solid State* **49** No 4, 691 (2007).
10. V.P. Gribkovskiy, *Theory of Absorption and Emission of Light in Semiconductors* (Minsk: Nauka i Tekhnika, 1975).
11. N.S. Averkiev, L.P. Kazakova, E.A. Lebedev, Yu.V. Rud', A.N. Smirnov, N.N. Smirnova, *Semicond.* **34** No 6, 732 (2000).
12. P.V. Zhukovskii, Ya. Partyka, P. Vengerek, Yu.V. Sidorenko, Yu.A. Shostak, A. Rodzik, *Semicond.* **35** No 8, 900 (2001).
13. *Optical Properties of Semiconductors: a Handbook* (V.I. Gavrilenko, A.M. Grehov, D.V. Korbutyak, V.G. Litovchenko) (Kiev: Naukova Dumka, 1987).
14. V.P. Makhniy, V.M. Sklyarchuk, Patent of Ukraine UA N108438, published 11.07.2016.
15. A.L. Fahrenbruch, R.H. Bube, *Fundamentals of Solar Cells, Photovoltaic Solar Energy Conversion* (New York: Academic Press, 1983).